Curve Enhancement Using Orientation Fields

Kristian Sandberg

Computational Solutions, LLC
1800 30th St. Suite 210B, Boulder, CO 80301

Abstract. We present a new method for enhancing the contrast of curve-like structures in images, with emphasis on Transmission Electron Microscopy tomograms of biological cells. The method is based on the Orientation Field Transform, and we introduce new techniques for generating directions and weights of the orientation field. The new method for generating the orientation field focuses on analyzing local asymmetries in the image. We demonstrate that analyzing geometric attributes such as orientations and symmetries results in a robust method that is relatively insensitive to poor and non-uniform contrast.

1 Introduction

Transmission Electron Microscopy (TEM) is a powerful tool to better understand structure and functionality of biological cells [1]. By imaging a specimen from multiple angles, tomographic reconstructions (tomograms) provide 3D images of cellular structures. In order to build easily viewable models of cellular structures, structures of interest are often segmented and rendered as surfaces.

Automating the segmentation process has proved difficult, and in most cases the user has to rely on manual segmentation tools such as IMOD [2]. Building 3D models using manual segmentation tools is often a slow and tedious process, sometimes requiring months of manual identification of cellular structures.

Due to the anisotropic resolution of TEM tomograms of cells [3], segmenting a 3D tomogram is often done slice-wise in the plane of highest resolution. In such slices, the cross section of structures often appear as curve-like structures.

In this paper we consider the problem of enhancing the contrast of curve-like structures in slices of 3D tomograms. Once the contrast of such structures has been enhanced, one can use thresholding and thinning operations to extract contours. This paper will focus on the contrast enhancement step while referring to the extensive literature for the thresholding/thinning problem (see [4] and references therein).

More specifically, we consider the following problem: *Given a 2D image and a scale parameter r, generate an image where the contrast of curve-like structures of thickness $\sim r$ are enhanced, while the contrast of non-curve-like structures are decreased.*

A major obstacle for adaptation of automated segmentation algorithms for cell biology is ¨the curse of parametrization¨. Many segmentation algorithms rely on several parameters to be tuned in order to obtain satisfactory results.

G. Bebis et al. (Eds.): ISVC 2009, Part I, LNCS 5875, pp. 564–575, 2009.

Tuning such parameters can be both time consuming and frustrating, especially in cases where the parameters lack intuitive meaning. We therefore consider minimizing the number of parameters of the segmentation process a priority.

Popular automated segmentation methods include Active Contours [5], Level Set methods [6], and the Watershed Transform [7]. Although these methods quite successfully detect compartment-like structures, they are less suitable for detecting curve-like objects [8]. In recent years there has also been an increasing interest in so-called eigenvector techniques [9],[10], which are flexible and can be tuned to detect curve-like structures.

Despite significant research in automatic segmentation techniques, few methods have proved useful for TEM tomograms of cells since these often suffer from low and non-uniform contrast, low signal to noise ratio, and also the presence of interfering structures [11],[8]. In this paper, interfering structures refer to high contrast structures of different shape attributes than the ones the segmentation algorithm targets (see Figure 1).

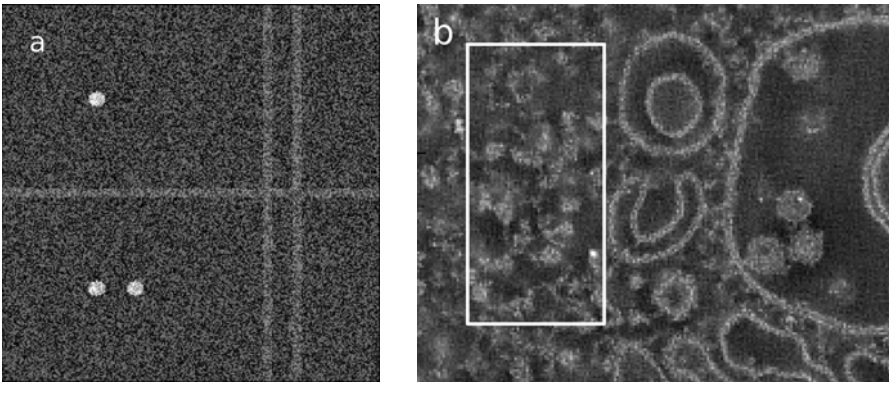

Fig. 1. a) A synthetically generated example where the goal is to detect the horizontal line and the two vertical lines. The dots are considered interfering structures. b) Slice of a tomogram of a Trypanosome. The structures inside the rectangle are examples of what we will refer to as interfering structures.

To address the problem of low and non-uniform contrast while enhancing curve-like structures, *orientation fields* have proved useful, particularly for finger print segmentation and matching [12], and for segmenting slices of tomograms of cells [11]. The orientation field is an assignment of a weighted line segment to each pixel in the image (see Figure 2). Each orientation has two attributes: an angle (ranging between 0 and 180 degrees), and a weight indicating the importance of the orientation. The orientation field can show remarkable uniformity even in cases where the contrast is highly non-uniform (see Figure 3 in [11]).

When using orientation fields for enhancing curve-like objects there are two main questions that have to be addressed: 1) How to generate the orientation field, and 2) how to detect curve-like objects in the orientation field. In this paper,

we will focus on the first question and use the Orientation Field Transform (OFT) [11] to detect curve-like objects once the orientation field has been generated.

A common method for generating the orientation field is to compute eigenvectors of the structure tensor [13], or some type of gradient [14], often combined with denoising. In 3D data sets, convolution-based edge detection methods have been described in, e.g., [15] and [16]. In [11], the authors used an approach based on line integration rather than differentiation, which turns out to be relatively stable for the challenging properties of TEM tomograms. However, the approach in [11] has several shortcomings, particularly in the presence of interfering structures.

In this paper, we develop new techniques for generating more robust weights for the orientation field that will properly reflect the reliability of the orientation. We also develop a new robust method for generating orientation directions. These improvements will lead to a robust method for enhancing curve-like objects, while leaving only one parameter, the scale r, for the user to adjust.

Although we will focus on segmentation of curve-like biological structures of TEM images, we note that our approach is general and can be used to enhance curve-like objects in any image. However, we have found TEM tomograms of cells to provide particularly challenging test data sets and therefore an excellent testing environment for image enhancement algorithms.

We review the definition of orientation fields and the OFT in Section 2 and also illustrate where the method for generating the orientation field in [11] fails. In Section 3 we present new techniques for generating a more robust orientation field, and enhance curve-like structures of a synthetic example and a slice from a real TEM tomogram in Section 4. We conclude the paper with a discussion of our approach and mention some of its limitations and future research.

2 Review of Orientation Fields and the OFT

Throughout this paper, we let $I(\mathbf{x})$ denote the image to be processed such that $I(\mathbf{x})$ gives the (gray scale) intensity at location $\mathbf{x} = (x, y)$. We will assume that targeted structures have a locally higher intensity than the background.

We define an orientation $\mathcal{F}$ as the tuple $\{w, \theta\}$ where θ is a direction that ranges between 0 and 180° and w is a positive weight indicating the importance of the direction. An orientation field $\mathcal{F}(\mathbf{x}) = \{w(\mathbf{x}), \theta(\mathbf{x})\}$ is the assignment of an orientation to each location in the image. We can illustrate the orientation field of an image by drawing a line segment at each pixel location, and vary its intensity to indicate the weights (see Figure 2).

To generate the orientation field, we consider the line integral operator

$$R[I](x, y, \theta) \equiv \int_{-\frac{r}{2}}^{\frac{r}{2}} I(x + s\cos\theta, y + s\sin\theta)\ ds, \tag{1}$$

where r is a scale parameter. This line integral computes the total intensity along a straight line of length r and direction θ centered at pixel (x, y).

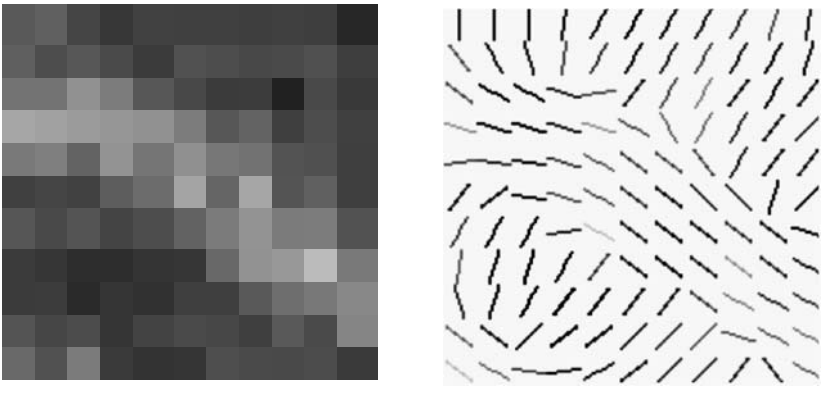

Fig. 2. The orientation field (right) of the image (left)

In [11], the orientation field was generated by

$$\mathcal{F}(x,y) = \left\{ \max_{\theta_k} R[I](x,y,\theta_k),\ \arg\max_{\theta_k} R[I](x,y,\theta_k) \right\} \tag{2}$$

for a sequence of equally spaced angles $\{\theta_k\}_{k=1}^{N_\theta}$ in the range $[0,\pi)$, where r was chosen as approximately two times the width of a typical curve-like structure in the image.

This definition has the advantage of being relatively insensitive to noise compared to gradient based methods for orientation field generation [17],[8]. However, it has some disadvantages that we will now discuss.

First, the orientation field near a structure tends to align with the structure, rather than perpendicularly to the structure, see Figure 3a and b. This happens since the integral along a line that cuts a structure diagonally will give a larger response than an integral along a line that cuts a structure perpendicularly. However, we shall see below that when using the OFT to detect curve-like structures in the orientation field, it is crucial that orientations align *parallel* to the curve for locations *inside* the curve, and align *perpendicular* to the curve for locations near but *outside* curves.

Secondly, the weights of the orientation field may be large even when located at or near a point-like structure, as illustrated in Figure 3d. Ideally, the orientation weights should be close to zero in such case, since these orientations are not associated with a curve-like structure.

In order to to detect curve-like structures in the orientation field, we will use the *Orientation Field Transform* (OFT). To this end, we first define the alignment integral operator Ω of the orientation field $\mathcal{F}(x,y)$ as

$$\Omega[\mathcal{F}](x,y,\alpha) = \tag{3}$$
$$\int_{-\frac{r}{2}}^{\frac{r}{2}} w(x+s\cos\alpha, y+s\sin\alpha)\cos\left(2(\theta(x+s\cos\alpha, y+s\sin\alpha)-\alpha)\right)\ ds$$

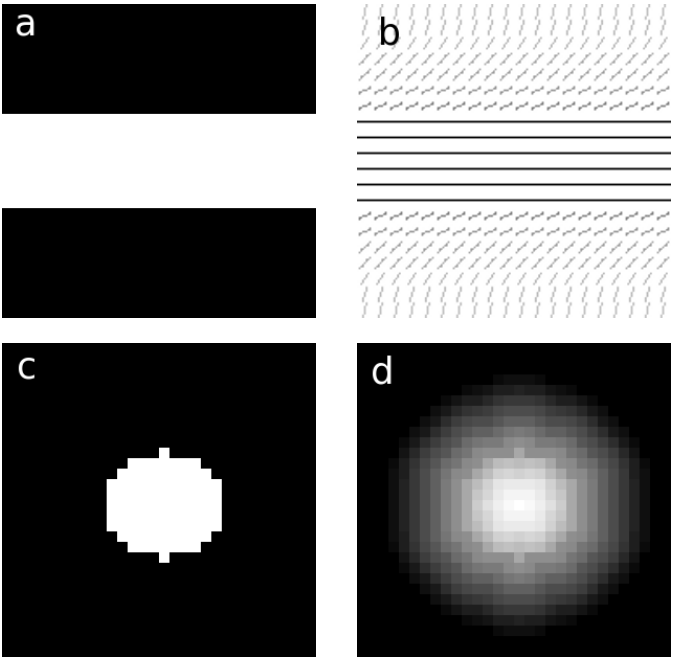

Fig. 3. a) A synthetically generated line-like structure. b) Orientation field for the structure in a) generated by the method in [11]. c) A synthetically generated point-like structure. d) Density plot of the orientation field weights for the structure in c) generated by the method in [11].

where α is an angle between 0 and 180°. This operator integrates the weights of the orientation field along straight lines through each pixel, multiplied by the alignment factor $\cos(2(\theta - \alpha))$. This alignment factor attains its maximum value 1 when θ and α are equal (parallel alignment), and attains it minimum value -1 when θ and α differ by 90° (perpendicular alignment).

To compute the OFT, we first search for the direction in which we have the strongest alignment (parallel or perpendicular), followed by evaluating the alignment integral Ω along the direction of strongest alignment. Formally, we define the OFT, $\mathcal{O}$, of the orientation field $\mathcal{F}(\mathbf{x}) = \{w(\mathbf{x}), \rho(\mathbf{x})\}$ as

$$\mathcal{O}[\mathcal{F}](\mathbf{x}) = \Omega[\mathcal{F}](\mathbf{x}, \tilde{\theta}), \quad \tilde{\theta} = \arg\max_{\alpha_k} |\Omega[\mathcal{F}](\mathbf{x}, \alpha_k)| \ .$$

We note that this operator generates a large negative response near a curve where the orientations (ideally) are aligned perpendicular to the curve, and large positive response inside a curve where the orientations (ideally) are aligned parallel along the curve. Since negative response indicates the exterior of a curve, we can therefore set $\mathcal{O}[\mathcal{F}](\mathbf{x})$ to zero at locations where the OFT response is negative. For examples and details, see [11].

3 A New Method for Generating Orientation Fields

In this section we address the shortcomings listed in Section 2 above. To this end, it will be convenient to introduce operators W and Θ, which extract the weight and direction from an orientation, that is, $\Theta(\mathcal{F}) = \theta$ and $W(\mathcal{F}) = w$.

3.1 Stable Generation of Orientation Field Direction

To generate directions that point perpendicular to a nearby curve, we introduce the notion of an ¨average¨ orientation. In order to compute the average of a collection of orientations, we need an addition algorithm for orientations that is associative (order independent). One way to do this, is to map each orientation to a vector in 2D represented in polar coordinates by doubling the direction angle such that $\{w, \theta\}$ is mapped to $\{w, 2\theta\}$. This mapping provides an invertible mapping between orientations and vectors in the plane. Since vector addition in the plane is associative, we can use the following algorithm for adding orientations $\{w_1, \theta_1\}$ and $\{w_2, \theta_2\}$:

1. Map orientations to 2D vectors:
   $\{w_1, \theta_1\} \mapsto \{w_1, 2\theta_1\} \equiv \mathbf{v_1}$ and $\{w_2, \theta_2\} \mapsto \{w_2, 2\theta_2\} \equiv \mathbf{v_2}$
2. Compute $\mathbf{v_{sum}} = \mathbf{v_1} + \mathbf{v_2}$ using the usual rules for vector addition and write the vector $\mathbf{v_{sum}}$ in its polar representation $\{w_{sum}, \theta_{sum}\}$.
3. Map the vector $\mathbf{v_{sum}}$ to an orientation: $\{w_{sum}, \theta_{sum}\} \mapsto \{w_{sum}, \theta_{sum}/2\}$

In particular, we see that two orientations with directions 90° apart and identical weights, add to a zero orientation (orientation with $w = 0$). For an alternative averaging algorithm (which can be generalized to higher dimensions), see [17].

Using the rules for orientation addition, we generate the direction of the orientation field of the image I as

$$\theta(x, y) = \Theta\left(\sum_{k=1}^{N_\theta} \{R[I](x, y, \theta_k),\ \theta_k\}\right) \tag{4}$$

where R is the line integral operator defined in (1) above. This definition differs to the one used in [11], by averaging over the response in different directions, rather than looking for the direction of maximum response. This means that outside a curve, the response will average (because of symmetry), to generate a net orientation perpendicular to the edge (see Figure 4).

3.2 Generation of Orientation Weights

In order to address the problems with orientation weights discussed in Section 2, we will consider two attributes that we refer to as *reliability* and *asymmetry alignment*. We will then use a simple fuzzy system to combine these two attributes to a single weight. One could add even more attributes, but we limit ourselves to only two since these two attributes are fairly general and should therefore work for a broad class of images.

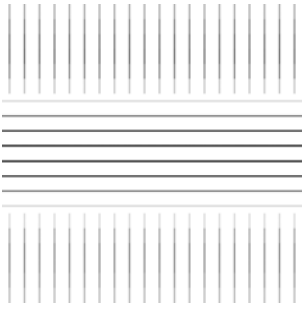

Fig. 4. The orientation field generated by (4) for the structure in Figure 3a

The Reliability Measure. The reliability measure, which we denote as $w_r(\mathbf{x})$, is given by extracting the weight from the sum computed for generating the direction in Section 3.1, that is,

$$w_r(\mathbf{x}) = W\left(\sum_{k=1}^{N_\theta} \{R[I](\mathbf{x}, \theta_k),\ \theta_k\}\right). \tag{5}$$

This expression is best understood by considering the response at the center of a radially symmetric point, in which case the response of the line integral $R[I](\mathbf{x}, \theta)$ is the same in all directions. By symmetry, the sum over orientations will therefore sum to the zero orientation, which we illustrate in Figure 5a.

The Asymmetry Alignment Measure. To prevent large orientation weights nearby point-like objects we observe that the absolute value of the 2D Fourier transform of an image of a radially symmetric point is symmetric, whereas the 2D Fourier transform of a line is highly asymmetric. By computing a local Fourier transform of an area centered at each pixel and analyzing the asymmetry of the resulting Fourier transformed data, we can measure ¨how curve-like¨ the neighborhood is.

To formalize these ideas, we first define the following data set

$$\tilde{I}(x, y, \xi, \eta) = \left| \int_{x-\frac{r}{2}}^{x+\frac{r}{2}} \int_{y-\frac{r}{2}}^{y+\frac{r}{2}} I(x', y') e^{-2\pi i(x'\xi + y'\eta)}\ dx'\ dy' \right|.$$

This operator computes the absolute value of the 2D Fourier transform of an r-by-r neighborhood of each pixel (x, y).

The asymmetry alignment measure w_a is defined by measuring the asymmetry of $\tilde{I}$ with respect to the (ξ, η) variables, and measuring the alignment of this asymmetry with the orientation direction:

$$w_a(x, y) = \sum_{k=1}^{N_\theta} \left(\int_{-\frac{r}{2}}^{\frac{r}{2}} \tilde{I}(x, y, s\cos\phi_k, s\sin\phi_k)\ ds \right) \cos(2(\phi_k - \theta(x, y) - \frac{\pi}{2})) \tag{6}$$

where $\{\phi_k\}_{k=1}^{N_\theta}$ is a set of equally spaced angles in the interval $[0, \pi)$.[1]

[1] The shift $\frac{\pi}{2}$ is needed since the 2D Fourier transform of a curve orientated at θ degrees in the space domain, will be oriented at $\theta - \frac{\pi}{2}$ degrees in the Fourier domain.

The purpose of this asymmetry measure is twofold. First, it measures the ¨strength¨ of the asymmetry.[2] Secondly, it measures the alignment of the asymmetry with the orientation direction computed in (4).

As an example, consider the value of $w_a(\mathbf{x})$ at a line structure with orientation θ. The line integral $\int_{-\frac{r}{2}}^{\frac{r}{2}} \tilde{I}(\mathbf{x}, s\cos\phi_k, s\sin\phi_k)\ ds$ attains it maximum value for $\phi_k = \theta - \pi/2$, for which the alignment factor $\cos(2(\phi_k - \theta - \frac{\pi}{2}))$ attains it maximum value. Hence, w_a will be large and positive at a line structure.

As a second example consider the response at (or near) a radially symmetric point. Since the 2D Fourier transform of a radially symmetric dot is radially symmetric, all terms in (6) cancel out. Hence, w_a is zero at or near a point structure.

As a final example, consider the response outside a straight line. Since we are measuring the absolute value of the asymmetry in the Fourier domain, the measure is independent of spatial shifts of the structure. Hence, the response of $\int_{-\frac{r}{2}}^{\frac{r}{2}} \tilde{I}(\mathbf{x}, s\cos\phi_k, s\sin\phi_k)\ ds$ attains it maximum value for the same ϕ_k as if located at the line structure. However, the orientation θ near but outside a line structure will be perpendicular to the line structure (Figure 4). Hence, $\phi_k = \theta_k$, for which the alignment factor $\cos(2(\phi_k - \theta - \frac{\pi}{2}))$ attains it minimum value (-1). Hence, w_a will be negative outside a line structure.[3]

In Figure 5b we display the weights w_a for the image in Figure 1a.

Combining the Reliability and the Asymmetry Alignment Measures. In order for a pixel to be associated with a curve-like object, we require large reliability response (w_r) and large asymmetry alignment response (w_a). Although there are many ways of combining these measures into a single weight, we have chosen the following criteria for simplicity: We first rescale $w_r(\mathbf{x})$ and $w_a(\mathbf{x})$ to the interval $[0, 1]$ by $w_r(\mathbf{x}) = \frac{w_r(\mathbf{x}) - \min_{\mathbf{x}} w_r(\mathbf{x})}{\max_{\mathbf{x}} w_r(\mathbf{x}) - \min_{\mathbf{x}} w_r(\mathbf{x})}$ and similarly for w_a. We then define $w(\mathbf{x}) = w_a(\mathbf{x})w_r(\mathbf{x})$ (element-wise multiplication when the weights are represented as matrices), which can be thought of as a simple fuzzy system [18]. We choose this criteria because of its simplicity, and since it does not introduce any additional parameters. In Figure 5c we display the weights w for the image in Figure 1a.

3.3 Summary of the Algorithm

We summarize the curve enhancement algorithm as follows:[4]

---

[2] One can obtain a more intensity independent measure by first setting $\tilde{I}(x, y, 0, 0) = 0$, that is setting the DC component (or zero frequency) to zero, before computing the sum in (6).

[3] Since negative response indicates the exterior of a curve, we can therefore set $w_a(\mathbf{x})$ to zero at locations where the response of (6) is negative.

[4] Note that all integrals are assumed to be approximated by sums.

1. Generate the orientation field:
   (a) For each location $\mathbf{x}$:
      i. Generate the directions $\theta(\mathbf{x})$ by using (4).
      ii. Generate the weights $w_r(\mathbf{x})$ by using (5).
      iii. Generate the weights $w_a(\mathbf{x})$ by using (6). If $w_a(\mathbf{x}) < 0$, set $w_a(\mathbf{x}) = 0$.
   (b) Rescale $w_r(\mathbf{x})$ and $w_a(\mathbf{x})$ to $[0, 1]$.
   (c) For each location $\mathbf{x}$: Compute $w(\mathbf{x}) = w_r(\mathbf{x})w_a(\mathbf{x})$.
2. Compute the OFT. For each location $\mathbf{x}$:
   (a) Compute the OFT by using (3).
   (b) If $\mathcal{O}[I](\mathbf{x}) < 0$, set $\mathcal{O}[I](\mathbf{x}) = 0$.

4 Results

We first verify the consistency of our algorithm by enhancing the line structures in Figure 1a. Although this is obviously a synthetic example, it provides valuable verification of our algorithm's ability to handle noise, and also of its ability to enhance the weak line-like structures while decreasing the contrast of the strong point-like structures as shown in Figure 5d. We used a scale parameter r corresponding to approximately 1.5 times the thickness of the line-like structures.

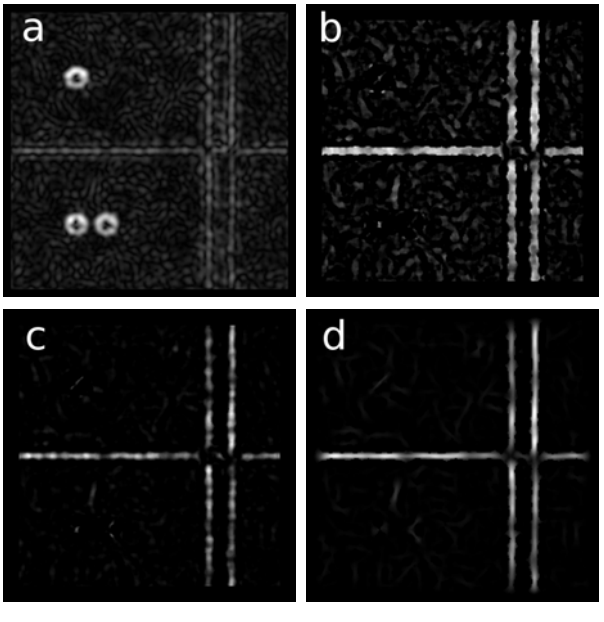

Fig. 5. Illustration of the orientation field weights for the image in Figure 1a displayed as density plots. a) The weights w_r. b) The weights w_a. c) The final weights. d) Result of applying the algorithm in Section 3.3 to the image in Figure 1a.

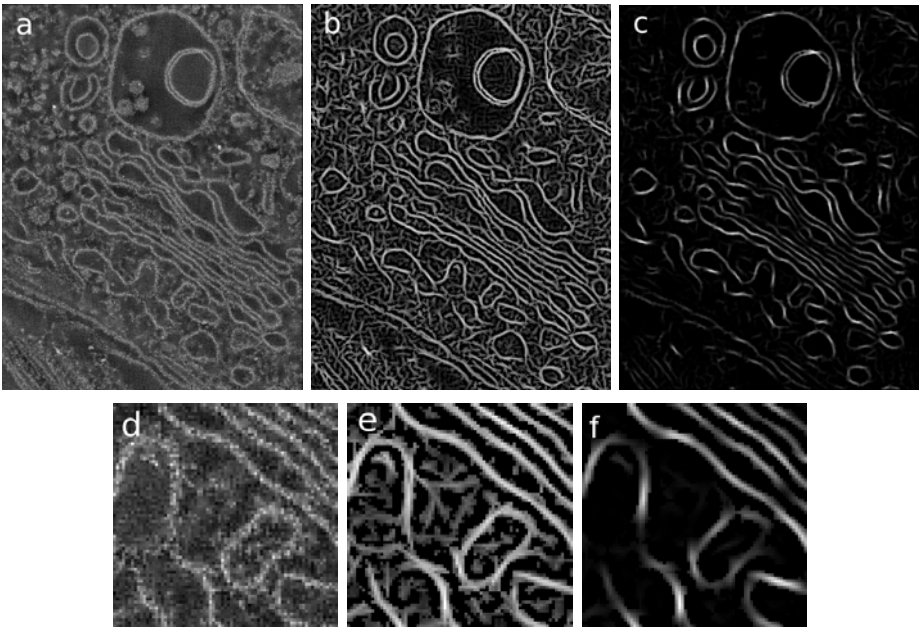

Fig. 6. Enhancement of a tomogram slice of a Trypanosome. a) Original image b) Result using the orientation field generated by the algorithm [11]. c) Result using the algorithm in Section 3.3. d) Closeup of the original image. e) Closeup of the result in b). f) Closeup of the result in c).

We next apply our algorithm to a slice from a real TEM tomogram[5] (Figure 6). In the left column we show the original image, in the center column the result when using the orientation field generated by the algorithm in [11], and in the right column the result of using our algorithm. We used a scale parameter r that corresponds to approximately 1.5 times the thickness of a typical membrane.

5 Discussion

Whereas many traditional segmentation methods focus on detecting edges and local correlation in texture, attributes which are known to be sensitive to nonuniform contrast and noise, the OFT detects correlations in geometrical attributes. However, in order for the OFT to be robust, it is essential for the orientation field to be based on attributes that are insensitive to contrast variations.

The method for generating the orientation field in [11] is relatively insensitive to noise, but still highly dependent on intensity and therefore sensitive to the presence of strong point-like structures. This problem can be partially remedied by locally smoothing the orientation field, thresholding, and allowing different

[5] Tomogram of Trypanosome, courtesy of Mary Morphew, the Boulder Laboratory for 3D Electron Microscopy of Cells, University of Colorado at Boulder.

scale parameters r_1 and r_2 to be used in (2) and (3), respectively. However, this requires more parameters to be tuned.

The methodology in this paper generates a significantly less contrast dependent orientation field by focusing more on local asymmetries than local intensities, and only requires one parameter to be set.

In order for a segmentation algorithms to be used routinely in a laboratory, experience shows that it is essential to minimize the number of parameters for the user to tune, and ensure that existing parameters have intuitive interpretations. The scale parameter used for the algorithm in this paper is easy to estimate as it is directly related to the thickness of a target structure.

We also point out that the suggested algorithm can be extended with more parameters. For example, one can introduce more attributes for generating the weights, and combine these using fuzzy logic, possibly within a neural network framework to train the fuzzy system.

In order to extend the current algorithm to detect objects with varying thickness and curvature, one should introduce a multiscale methodology by simultaneously process the data for a range of scale parameters r combined with some criteria on how to locally select r. We also note that the OFT currently uses a family of straight lines of fixed length to search for correlation in the orientation field. A more sophisticated version can use a family of curves of varying curvature as well, which should improve the accuracy for finding structures with large curvatures.

Finally, we plan on extending the current work to detect curves and planes in 3D data sets.

6 Conclusion

We have refined an earlier suggested method for enhancing the contrast of curve-like structures in TEM tomograms. The method is based on the Orientation Field Transform, but uses a more robust technique to generate the orientation field of an image compared to earlier suggested methods. The resulting method is stable both with respect to noise and presence of high contrast point-like objects. Furthermore, the algorithm only requires one parameter to be set by the user, and is therefore easy to use.

Acknowledgment

The author would like to thank Alejandro Cantarero for his valuable comments and suggestions.

References

1. Richard McIntosh, J. (ed.): Methods in Cell Biology: Cellular Electron Microscopy, vol. 79. Elsevier Inc., Amsterdam (2007)
2. Kremer, J.R., Mastronarde, D.N., McIntosh, J.R.: Computer visualization of three-dimensional image data using IMOD. J. Struct. Biol. 116, 71–76 (1996)

3. Penczek, P., Marko, M., Buttle, K., Frank, J.: Double-tilt Electron Tomography. Ultramicroscopy 60, 393–410 (1995)
4. Gonzales, R.C., Woods, R.E.: Digital Image Processing, 3rd edn. Prentice Hall, Englewood Cliffs (2007)
5. Chan, T.F., Vese, L.A.: Active Contours Without Edges. IEEE Trans. Image Processing 10(2), 266–277 (2001)
6. Osher, S., Fedkiw, R.: Level Set Methods and Dynamic Implicit Surfaces. Springer, Heidelberg (2003)
7. Volkmann, N.: A Novel Three-dimensional Variant of the Watershed Transform for Segmentation of Electron Density Maps. J. Struct. Biol. 138, 123–129 (2002)
8. Sandberg, K.: Methods for Image Segmentation in Cellular Tomography. In: McIntosh, J.R. (ed.) Methods in Cell Biology: Cellular Electron Microscopy, vol. 79, pp. 769–798. Elsevier Inc., Amsterdam (2007)
9. Frangakis, A.S., Hegerl, R.: Segmentation of Two- and Three-dimensional Data from Electron Microscopy Using Eigenvector Analysis. Journal of Structural Biology 138, 105–113 (2002)
10. Coifman, R.R., Lafon, S., Lee, A.B., Maggioni, M., Nadler, B., Warner, F., Zucker, S.W.: Geometric Diffusions as a Tool for Harmonic Analysis and Structure Definition of Data, Part I: Diffusion Maps. Proc. Natl. Acad. Sci. USA 102(21), 7426–7431 (2005)
11. Sandberg, K., Brega, M.: Segmentation of Thin Structures in Electron Micrographs Using Orientation Fields. J. Struct. Biol. 157, 403–415 (2007)
12. Gu, J., Zhou, J.: A Novel Model for Orientation Field of Fingerprints. In: Proceedings of the 2003 IEEE Computer Society Conference on Computer Vision and Pattern Recognition, vol. 2, pp. 493–498 (2003)
13. Weickert, J.: Anisotropic Diffusion in Image Processing. Teubner-Verlag (1998)
14. Kass, M., Witkin, A.: Analyzing Oriented Pattern. In: Computer Vision, Graphics and Image Processing, vol. 37, pp. 362–397 (1987)
15. Zucker, S.W., Hummel, R.A.: A Three-dimensional Edge Operator. IEEE Trans. Pattern Analysis 3(3), 324–331 (1981)
16. Pudney, C., Kovesi, P., Robbins, B.: Feature Detection Using Oriented Local Energy for 3D Confocal Microscope Images. In: Chin, R., Naiman, A., Pong, T.-C., Ip, H.H.-S. (eds.) ICSC 1995. LNCS, vol. 1024, pp. 274–282. Springer, Heidelberg (1995)
17. Brega, M.: Orientation Fields and Their Application to Image Processing. Master's thesis, University of Colorado at Boulder (2005)
18. Ross, T.J.: Fuzzy Logic with Engineering Applications, 2nd edn. Wiley, Chichester (2004)